

# In Silico Estimation of Skin Concentration Following the Dermal Exposure to Chemicals

Tomomi Hatanaka<sup>1</sup> · Shun Yoshida<sup>2</sup> · Wesam R. Kadhum<sup>2</sup> · Hiroaki Todo<sup>2</sup> · Kenji Sugibayashi<sup>2</sup>

Received: 13 April 2015 / Accepted: 10 July 2015 / Published online: 21 July 2015  
© Springer Science+Business Media New York 2015

## ABSTRACT

**Purpose** To develop an *in silico* method based on Fick's law of diffusion to estimate the skin concentration following dermal exposure to chemicals with a wide range of lipophilicity.

**Methods** Permeation experiments of various chemicals were performed through rat and porcine skin. Permeation parameters, namely, permeability coefficient and partition coefficient, were obtained by the fitting of data to two-layered and one-layered diffusion models for whole and stripped skin. The mean skin concentration of chemicals during steady-state permeation was calculated using the permeation parameters and compared with the observed values.

**Results** All permeation profiles could be described by the diffusion models. The estimated skin concentrations of chemicals using permeation parameters were close to the observed levels and most data fell within the 95% confidence interval for complete prediction. The permeability coefficient and partition coefficient for stripped skin were almost constant, being independent of the permeant's lipophilicity.

**Conclusions** Skin concentration following dermal exposure to various chemicals can be accurately estimated based on Fick's law of diffusion. This method should become a useful tool to assess the efficacy of topically applied drugs and

cosmetic ingredients, as well as the risk of chemicals likely to cause skin disorders and diseases.

**KEY WORDS** dermal exposure · Fick's law of diffusion · *in silico* · skin concentration · skin permeation

## ABBREVIATIONS

$\bar{C}_{ss}$	Mean concentration in stripped skin during steady-state permeation
$\bar{C}_{ws}$	Mean concentration in whole skin during steady-state permeation
$K_{sc}$	Stratum corneum/donor vehicle partition coefficient
$K_{ss}$	Stripped skin/donor vehicle partition coefficient
$P_{ss}$	Permeability coefficient through stripped skin
$P_{ws}$	Permeability coefficient through whole skin
AMP	Aminopyrine
ANP	Antipyrine
BA	Benzoic acid
BP	Butyl <i>p</i> -hydroxybenzoate
B-PABA	Butyl 4-aminobenzoate
CAF	Caffeine
ClogP	Calculated LogP
Dopa	Dopamine hydrochloride
EP	Ethyl <i>p</i> -hydroxybenzoate
E-PABA	Ethyl 4-aminobenzoate
Epi	Epinephrine hydrochloride
LC	Lidocaine hydrochloride
LogP	Logarithm of <i>n</i> -octanol/water partition coefficient
MP	Methyl <i>p</i> -hydroxybenzoate
M-PABA	Methyl 4-aminobenzoate
PP	Propyl <i>p</i> -hydroxybenzoate
P-PABA	Propyl 4-aminobenzoate

✉ Kenji Sugibayashi  
sugib@josai.ac.jp  
Tomomi Hatanaka  
tmmhtnk@tokai-u.jp

<sup>1</sup> Tokai University School of Medicine, 143 Shimokasuya Isehara, Kanagawa 259-1193, Japan

<sup>2</sup> Faculty of Pharmaceutical Sciences, Josai University, 1-1 Keyakidai Sakado, Saitama 350-0295, Japan

## INTRODUCTION

Since the Transderm-Scōp® patch was introduced onto the market more than three decades ago, thirty and more transdermal drug delivery systems have become available as therapeutic tools for a variety of diseases; further development of such systems is desirable as alternatives to oral formulations and hypodermic injections, especially for macromolecules and vaccines (1,2). Skin is one of the protective barriers against exogenous substances; only a limited number of drugs and toxins are capable of penetrating it (3). The estimation of systemic exposure after the absorption of any chemical through the skin is relevant to both the development of formulations for transdermal drug delivery and risk assessment of unintended contact with environmental materials. The final goal is the accurate prediction of skin permeability and blood concentration without experimental measurement; with this goal in mind, a number of *in silico* models have been reported in the literature, from quantitative relationships to mechanistic models (4–10).

Since ancient times, skin has been used as the administration site to obtain a localized pharmacological effect of drugs; even now, topical dermatological products are used in treating various skin disorders (11). Sunscreens and skin protective agents act at the surface of the skin, whereas the site of action is the viable epidermis and dermis for antimicrobials, NSAIDs, steroids, antipruritics and functional cosmetics. The skin concentration is more important than the skin permeation behavior for such topical drugs and cosmetic ingredients, as well as chemicals likely to cause skin disorders and diseases.

Many methods of measuring skin concentration have been reported, such as suction blister (12), punch and shave biopsies (13), heating (14), autoradiography (15), tape-stripping (16), microdialysis (17) and Raman spectrophotometry (18), but are unfortunately expensive and time-consuming. However, animal experiments have increasingly attracted criticism in terms of animal welfare (19). Scientists are now encouraged to follow the 3Rs principle, namely, to replace, reduce and/or refine laboratory animal use where possible. *In silico* models for estimating the skin concentration are desired in order to evaluate the efficacy and safety following dermal exposure to topically active compounds.

Because the primary resistance to skin permeation occurs at the stratum corneum, the skin's most superficial layer (20), a single-layer membrane has been assumed in most of the models assessing systemic exposure after the absorption of chemicals by the skin (5–8). This assumption is reasonable, except for extremely lipophilic permeants, for which the viable epidermis and dermis present a barrier against skin permeation (21). In actual fact, accurate predictive values of permeability coefficients for a wide range of chemicals have been obtained from the physicochemical parameters under the

assumption by Potts and Guy (6) as well as us (22). The viable epidermis and dermis, which occupy large volumes in the skin and are the sites of action for some chemicals, are not layers that can be ignored for the estimation of skin concentration. This is a reason why establishment of *in silico* estimation methods for skin concentration fell behind that for skin permeation of chemicals.

We previously demonstrated that the mean paraben (4-hydroxybenzoate) concentration in hairless rat skin during steady-state permeation could be predicted based on Fick's law of diffusion using permeation parameters obtained from a permeation experiment (23). This method is here expanded to estimating the concentration of chemicals with a wide range of lipophilicity in rat and porcine skins. With the aim of achieving complete *in silico* prediction without experimental measurement, the permeation parameters used in the estimation are related to  $ClogP$ , a predictor of the logarithm of the *n*-octanol/water partition coefficient ( $LogP$ ) (24). Since the permeation parameters for whole skin have already been related to  $LogP$  (22), we are particularly focusing on viable epidermis and dermis.

## MATERIALS AND METHODS

### Materials

Epinephrine hydrochloride (Epi), caffeine (CAF), antipyrine (ANP), aminopyrine (AMP) and benzoic acid (BA) were purchased from Wako Chemical Industries, Ltd. (Osaka, Japan). Methyl 4-aminobenzoate (M-PABA), ethyl 4-aminobenzoate (E-PABA), propyl 4-aminobenzoate (P-PABA), *n*-butyl 4-aminobenzoate (B-PABA), methyl 4-hydroxybenzoate (MP), ethyl 4-hydroxybenzoate (EP), propyl 4-hydroxybenzoate (PP) and *n*-butyl 4-hydroxybenzoate (BP) were from Tokyo Chemical Industry Co., Ltd. (Tokyo, Japan). Dopamine hydrochloride (Dopa) and lidocaine hydrochloride (LC) were from Sigma Aldrich (St. Louis, MO). Chemicals used as model permeants and their physicochemical properties are listed in Table I. Other chemicals and reagents were of special grade or HPLC grade, commercially obtained and used without further purification.

### Preparation of Skin Membranes

Male hairless rats (WBM/ILA-Ht, 8 weeks of age, body weight of 220–260 g) were obtained from the Life Science Research Center, Josai University (Sakado, Saitama, Japan), or Ishikawa Experimental Animal Laboratories (Fukaya, Saitama, Japan). Whole abdominal skin was freshly excised from hairless rats after being shaved carefully and cleaned with pH 7.4 PBS under pentobarbital (50 mg/kg, *i.p.*) anesthesia. The stripped skin was prepared by stripping stratum

**Table 1** Physicochemical Properties of Chemicals Used in this Study

Chemical	Molecular weight	pK <sub>a</sub>	ClogP
Epinephrine (Epi)	219.67	8.55 <sup>a</sup>	-0.68
Caffeine (CAF)	194.19	14.0 <sup>b</sup>	-0.04
Dopamine (Dopa)	189.64	8.89 <sup>a</sup>	0.17
Antipyrine (ANP)	188.23	2.20 <sup>b</sup>	0.20
Aminopyrine (AMP)	231.29	5.00 <sup>b</sup>	0.57
Methyl 4-aminobenzoate (M-PABA)	151.17	2.47 <sup>c</sup>	1.39
Methyl 4-hydroxybenzoate (MP)	152.15	8.40 <sup>b</sup>	1.56
Benzoic acid (BA)	122.12	4.20 <sup>a</sup>	1.88
Ethyl 4-aminobenzoate (E-PABA)	165.19	2.51 <sup>c</sup>	1.93
Lidocaine (LC)	234.36	7.86 <sup>b</sup>	1.95
Propyl 4-aminobenzoate (P-PABA)	179.22	2.49 <sup>c</sup>	2.45
Ethyl 4-hydroxybenzoate (EP)	166.18	8.40 <sup>b</sup>	2.51
n-Butyl 4-aminobenzoate (B-PABA)	193.24	2.47 <sup>c</sup>	2.98
Propyl 4-hydroxybenzoate (PP)	180.20	8.40 <sup>b</sup>	3.04
n-Butyl 4-hydroxybenzoate (BP)	194.23	8.40 <sup>b</sup>	3.57

ClogP, logarithm of octanol/water partition coefficient calculated using Chem Draw Ultra 12.2.2® (PerkinElmer Informatics, Cambridge, MA)

<sup>a</sup>, <sup>b</sup>, <sup>c</sup> Values reported in the literature (25–27)

corneum 20 times with cellophane tape (Cellotape® CT-15, Nichiban, Tokyo, Japan) prior to its excision from rats (28). All animal experiments were performed according to the ethics committee of Josai University.

Frozen ears of male and female pigs (LWD, 6–12 months) were purchased from ZEN-NOH Central Institute for Food and Livestock (Tsukuba, Ibaraki, Japan). The porcine ears were stored at -80°C and thawed at 32°C immediately before the skin permeation experiments. The whole skin was excised after being shaved carefully and cleaned with pH 7.4 PBS; stripped skin was made by tape-stripping the stratum corneum 30 times with adhesive tape prior to its excision from the porcine ear (29).

### Preparation of Donor Solutions

Donor solutions were prepared considering the solubility and dissociation of chemicals in aqueous solutions. Dopa and Epi were applied to skin in 100 mM citrate buffer solution (pH 5), BA was applied in 20 mM citrate buffer solution (pH 3) and LC was applied in 10 mM carbonate buffer solution (pH 10). The donor concentration in phosphate-buffered solutions (pH 7.4) was 100 mM for ANP, ISMN, CAF and AMP; 10 mM for MP and M-PABA; and 5 mM for BP and B-PABA. To avoid hydrolysis by esterase in skin, 0.54 mM diisopropyl fluorophosphate, a serine protease inhibitor, was included in the donor solutions for 4-hydroxybenzoates and 4-aminobenzoates (23). The chemicals except for Epi, CAF and Dopa existed in their unionized forms in the donor solutions.

### Skin Permeation Experiments

Skin permeation experiments were carried out to estimate the permeation parameters, namely, permeability coefficient and partition coefficient, of chemicals. Excess fat was trimmed off from the excised (whole or stripped) skin and the skin sample was set in a vertical-type diffusion cell (effective diffusion area, 1.77 cm<sup>2</sup>), in which the receiver chamber was warmed to 32°C. One mL of buffer solution, which corresponded to the donor solution and contained no permeant, was applied to the epidermis side and 6 mL of the buffer was applied to the dermis side of skin to reach an equilibration state for about 30 min (rat) and 1 h (pig). In the cases of 4-hydroxybenzoates and 4-aminobenzoates, the phosphate-buffered solutions (pH 7.4) containing 2.7 mM diisopropyl fluorophosphates were used for the complete inhibition of hydrolysis by esterase in skin. The buffer solutions of both epidermis and dermis sides were replaced with the same volumes of donor solution and fresh buffer solution (*i.e.*, receiver solution), respectively, in order to start the permeation experiment. The phosphate-buffered solutions (pH 7.4) containing 0.54 mM diisopropyl fluorophosphates were used as receiver solutions for 4-hydroxybenzoates and 4-aminobenzoates. The receiver solution was stirred with a stirrer bar on a magnetic stirrer and maintained at 32°C throughout the experiments. An aliquot (500 µL) was withdrawn from the receiver chamber and the same volume of fresh buffer solution was added to the chamber to keep the volume constant. The penetrant concentration in the receiver chamber was determined by HPLC.

### Determination of Skin Concentrations

The concentrations of chemicals in rat and porcine whole skin were measured during steady-state permeation, 4 and 24 h after the start of permeation experiments, which were performed separately from the experiments mentioned above. The donor solution was removed, the stratum corneum side was rinsed three times with 1.0 mL of appropriate buffer solution and then the chemical-applied area was cut out. When the concentrations in viable epidermis and dermis were measured, the stratum corneum was removed by tape-stripping before clipping out the application area. The piece of skin was minced with scissors and 0.5 mL of buffer solution was added prior to its homogenization at 12,000 rpm and 4°C for 5 min using a homogenizer (Polytron PT 1200 E, Kinematica AG, Littau-Lucerne, Switzerland). For the deproteinization, 0.5 mL of 16% trichloroacetic acid in buffer solution was added to the skin homogenate, followed by agitation at 32°C for 15 min, and then the mixture was centrifuged at 15,000 rpm and 4°C for 5 min. The chemical concentration in the resulting supernatant was determined by HPLC.

## HPLC Analysis

Samples were mixed with the same volume of acetonitrile containing an internal standard and centrifuged at 15,000 rpm and 4°C for 5 min. The obtained supernatant (10 or 20 µL) was injected into an HPLC system. The HPLC system (Shimadzu Co., Kyoto, Japan) consisted of a system controller (SCL-10A), pump (LC-20AD), degasser (DGU-20A<sub>3</sub>), auto-injector (SIL-20A), column oven (CTO-20A), UV detector (SPD-20A) and analysis software (LC Solution). The column was CAPCELL PAK C18 UG120 S5 4.6 mm × 150 mm (Shiseido Co., Tokyo, Japan) for Dopa and Epi, and Inertsil® ODS-3 4.6 mm × 150 mm (GL Sciences Inc., Tokyo, Japan) for the other chemicals. The column was maintained at 40°C and the flow rate of the mobile phase was adjusted to 1.0 mL/min in all cases. Other conditions are listed in Table II.

## Data Analysis

A two-layered diffusion model consisting of the stratum corneum and viable epidermis and dermis was employed in predicting the skin concentration following dermal exposure to chemicals (23). On the basis of this model, the mean concentrations of chemicals in whole skin ( $\overline{C}_{ws}$ ) and stripped skin ( $\overline{C}_{ss}$ ) during steady-state permeation can be represented as follows:

$$\overline{C}_{ws} = \frac{C_v}{2L_{ws}} \left\{ K_{sc}L_{sc} \left( 1 + \frac{P_{ws}}{P_{ss}} \right) + K_{ss}L_{ss} \frac{P_{ws}}{P_{ss}} \right\} \quad (1)$$

$$\overline{C}_{ss} = \frac{K_{ss}C_v}{2} \quad (2)$$

where  $C$ ,  $K$ ,  $P$  and  $L$  are the concentration, partition coefficient, permeability coefficient of chemicals and thickness of skin layers, and subscripts  $v$ ,  $ws$ ,  $sc$  and  $ss$  are the vehicle, whole skin, stratum corneum and stripped skin, in other words, viable epidermis and dermis, respectively. Permeation parameters required in predicting the skin concentration of chemicals were estimated by model adaptation of permeation data (30). The parameters for stripped skin ( $P_{ss}$  and  $K_{ss}$ ) were obtained by fitting permeation data through stripped skin to the one-layered diffusion model. Estimation of  $P_{ws}$  and  $K_{sc}$  values was carried out by fitting permeation data through whole skin to the two-layered diffusion model using previously obtained values of  $P_{ss}$  and  $K_{ss}$ . A weighted least-squares method based on a quasi-Newton algorithm, which was run on the solver-function of Microsoft Excel 2007, was used to estimate the permeation parameters. The mean steady-state concentrations ( $\overline{C}_{ws}$  and  $\overline{C}_{ss}$ ) were calculated by introducing the estimated values of permeation parameters and measured mean values of layer thickness ( $L_{ws}$  = 600 µm,  $L_{sc}$  = 15 µm,  $L_{ss}$  = 585 µm for rats,  $L_{ws}$  = 1500 µm,  $L_{sc}$  = 15 µm,  $L_{ss}$  = 1485 µm for pig) into Eqs. 1 and 2.

## RESULTS

### Calculation of Permeation Parameters

Permeation experiments of chemicals with various polarities through hairless rat and porcine skin were first performed to obtain the permeation parameters. Figure 1 shows the typical permeation profiles, a typical hydrophobic permeant, LC and a typical hydrophilic one, Dopa through whole and stripped skin of hairless rats. The corresponding data for porcine skin are shown in Fig. 2. The permeation properties such as permeation rate and lag time differed depending on the permeant and animal. Nevertheless, the permeation profiles through whole and stripped skin could be described by the two-layered and one-layered diffusion models, respectively. The permeation parameters of all model permeants could be obtained and are given in Table III.

### Estimation of Skin Concentration

Mean concentrations of chemicals in whole and stripped skin of rat and pig during steady-state permeation were estimated from Eqs. 1 and 2 using the permeation parameters calculated above. The estimated values were normalized by the applied (donor) concentration and compared with the observed values (Figs. 3 and 4). Most data for the two types of skin and animal fell within the 95% confidence interval for complete prediction, although the concentrations of Epi and Dopa were underestimated, especially in the whole skin of the both animals.

### Relationship Between Permeation Parameters and Lipophilicity

Figure 5 shows the relationships between the permeation parameters, permeability coefficient and partition coefficient of chemicals for rat stripped skin and  $\text{Clog}P$ . Each permeation parameter was almost constant, being independent of  $\text{Clog}P$ . A similar relationships were observed for porcine stripped skin (Fig. 6).

## DISCUSSION

In the present study, we established an *in silico* method for estimating skin concentration after dermal exposure to chemicals. We previously demonstrated that the mean paraben concentration in hairless rat skin during steady-state permeation could be predicted based on Fick's law of diffusion using parameters obtained from a permeation experiment (23). It is necessary to expand the application range, namely, to a variety of chemicals and skin types, for clinical use. Fifteen chemicals, with  $\text{Clog}P$  ranging from -0.68 to 3.6 and

**Table II** HPLC Conditions for Analysis of Chemicals Used in this Study

Chemical	Mobile phase	Detection wavelength (nm)	Internal standard
Epi	Acetonitrile:0.1% phosphoric acid (35:65)+ 5 mM sodium dodecylsulfate	280	— <sup>a</sup>
CAF	Acetonitrile:0.1% phosphoric acid (10:90)	254	— <sup>a</sup>
Dopa	Acetonitrile:0.1% phosphoric acid (35:65)+ 5 mM sodium dodecylsulfate	280	— <sup>a</sup>
ANP	Acetonitrile:water (20:80)	254	— <sup>a</sup>
AMP	Acetonitrile:0.1% phosphoric acid (50:50)+ 5 mM sodium dodecylsulfate	245	BP
M-PABA	Acetonitrile:0.1% phosphoric acid (30:70)	280	E-PABA
MP	Acetonitrile:0.1% phosphoric acid (30:70)	260	EP
BA	Acetonitrile:0.1% phosphoric acid (45:55)	254	EP
E-PABA	Acetonitrile:0.1% phosphoric acid (30:70)	280	M-PABA
LC	Acetonitrile:0.1% phosphoric acid (30:70)+ 5 mM sodium 1-heptanesulfate	230	— <sup>a</sup>
P-PABA	Acetonitrile:0.1% phosphoric acid (45:55)	254	EP
EP	Acetonitrile:0.1% phosphoric acid (30:70)	260	MP
B-PABA	Acetonitrile:0.1% phosphoric acid (45:55)	280	P-PABA
PP	Acetonitrile:0.1% phosphoric acid (45:55)	260	BP
BP	Acetonitrile:0.1% phosphoric acid (45:55)	260	PP

<sup>a</sup> Absolute calibration curve method was used

molecular weight from 122.12 to 234.30, were used as model permeants. In addition to hairless rat, pig was selected as a skin donor due to its skin's anatomical, physiological and biochemical similarities to human skin (31).

At the beginning of the present study, skin permeation experiments through whole and stripped skin of rats and pigs

were carried out to obtain the permeation parameters required for estimation of the chemical concentration in skin. Steady-state permeation was achieved after a short lag time for all experiments, but the permeation properties differed depending on the chemicals, skin types and animals (Figs. 1 and 2). LC permeation through whole skin of the two animals

**Fig. 1** Typical permeation profiles of LC and Dopa through whole (a, c) and stripped skin (b, d) of rats. Solid lines represent nonlinear least-squares fit of data to one- (b, d) and two-layered (a, c) diffusion models (23).

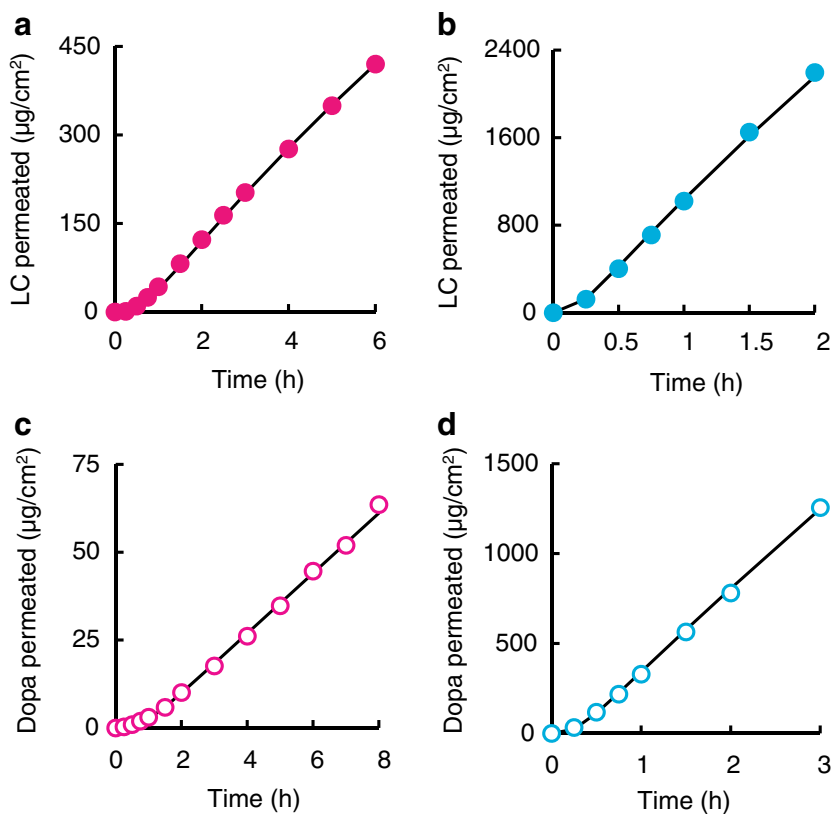
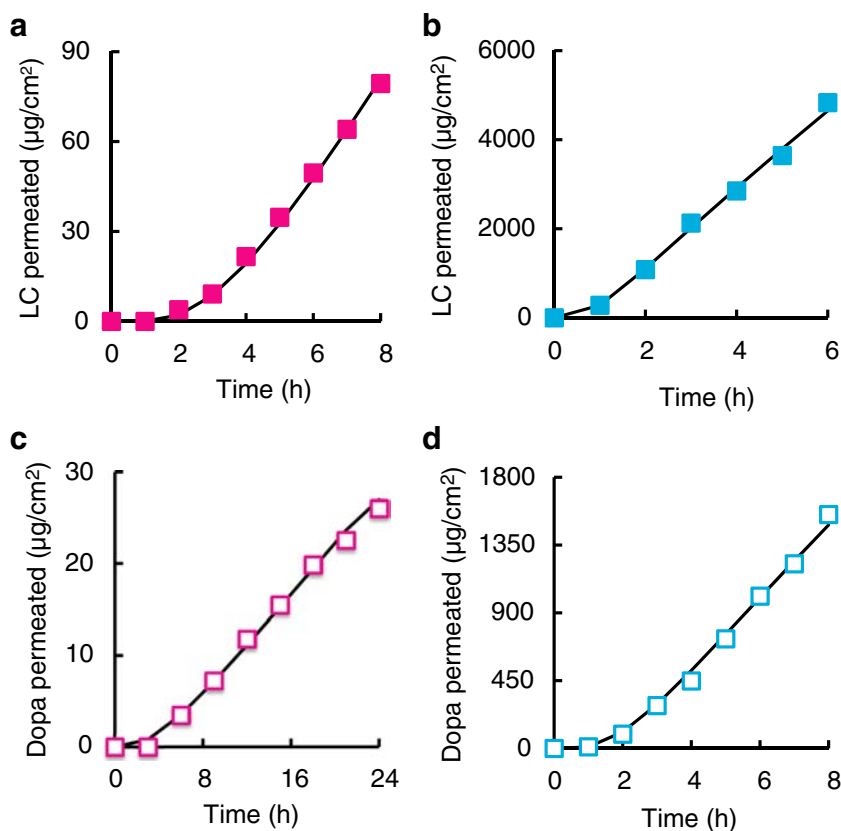


**Fig. 2** Typical permeation profiles of LC and Dopa through whole (a, c) and stripped skin (b, d) of pigs. Solid lines represent nonlinear least-squares fit of data to one- (b, d) and two-layered (a, c) diffusion models (23).



was higher than that for Dopa, although the donor concentration was ten times lower. Removal of stratum corneum

increased the permeation of chemicals, and its effect on hydrophilic Dopa was much greater than that on lipophilic LC.

**Table III** Permeation Parameters Estimated by Model Adaptation of Permeation Data of Chemicals

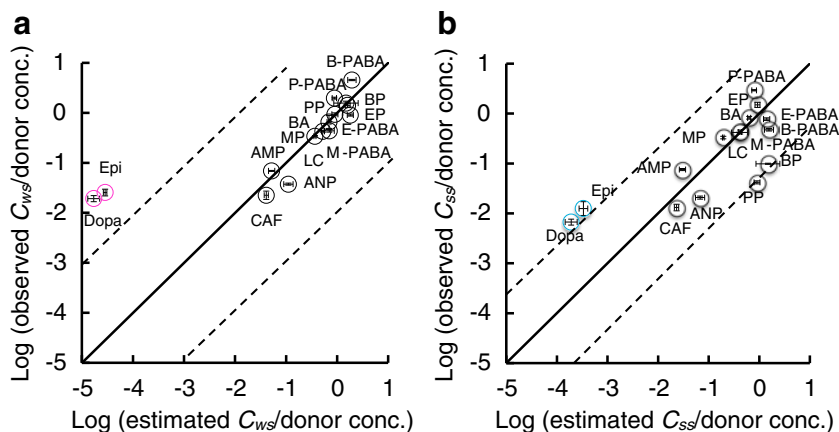
Chemicals	Hairless rat				Pig			
	$P_{ws}^b$ (cm/s)	$K_{sc}^b$	$P_{ss}^a$ (cm/s)	$K_{ss}^a$	$P_{ws}^b$ (cm/s)	$K_{sc}^b$	$P_{ss}^a$ (cm/s)	$K_{ss}^a$
Epi	$2.7 \times 10^{-7}$	0.70	$3.1 \times 10^{-4}$	0.64	$2.0 \times 10^{-8}$	0.5	$6.6 \times 10^{-6}$	2.4
CAF	$2.4 \times 10^{-7}$	0.50	$1.9 \times 10^{-5}$	0.55	$5.1 \times 10^{-8}$	0.4	$5.8 \times 10^{-6}$	0.87
Dopa	$1.3 \times 10^{-7}$	0.43	$1.9 \times 10^{-4}$	0.58	$1.2 \times 10^{-7}$	0.4	$3.9 \times 10^{-6}$	3.6
ANP	$2.2 \times 10^{-6}$	3.8	$1.6 \times 10^{-5}$	1.1	$1.5 \times 10^{-7}$	2.0	$7.5 \times 10^{-6}$	0.79
AMP	$2.7 \times 10^{-7}$	1.6	$1.2 \times 10^{-5}$	2.5	$1.4 \times 10^{-7}$	1.0	$5.4 \times 10^{-6}$	0.65
M-PABA	$1.5 \times 10^{-5}$	20	$3.6 \times 10^{-5}$	4.6	$2.6 \times 10^{-6}$	7.5	$1.0 \times 10^{-5}$	1.0
MP	$3.4 \times 10^{-6}$	14	$4.4 \times 10^{-5}$	4.9	$4.4 \times 10^{-6}$	25	$7.6 \times 10^{-6}$	1.3
BA	$1.3 \times 10^{-5}$	6.9	$5.8 \times 10^{-5}$	6.0	$7.2 \times 10^{-6}$	18	$1.4 \times 10^{-5}$	3.3
E-PABA	$1.7 \times 10^{-5}$	20	$2.9 \times 10^{-5}$	4.6	$2.8 \times 10^{-6}$	1.0	$7.9 \times 10^{-6}$	0.95
LC	$7.9 \times 10^{-6}$	7.0	$2.3 \times 10^{-5}$	2.4	$1.8 \times 10^{-6}$	1.5	$4.9 \times 10^{-6}$	0.65
P-PABA	$1.2 \times 10^{-5}$	6.0	$2.1 \times 10^{-5}$	3.3	$7.1 \times 10^{-6}$	7.0	$9.9 \times 10^{-6}$	2.7
EP	$7.9 \times 10^{-6}$	39	$2.5 \times 10^{-5}$	7.3	$5.0 \times 10^{-6}$	20	$5.8 \times 10^{-6}$	1.4
B-PABA	$4.9 \times 10^{-6}$	20	$5.0 \times 10^{-6}$	2.0	$4.1 \times 10^{-6}$	6.0	$5.0 \times 10^{-6}$	2.7
PP	$5.3 \times 10^{-6}$	1.5	$2.0 \times 10^{-5}$	5.8	$4.5 \times 10^{-6}$	10	$7.1 \times 10^{-6}$	2.8
BP	$5.5 \times 10^{-6}$	2.5	$9.6 \times 10^{-6}$	7.5	$2.6 \times 10^{-6}$	6.0	$4.0 \times 10^{-6}$	3.3

Each value represents the mean of 4 experiments

<sup>a</sup>The values were obtained by fitting permeation data through stripped skin to the one-layered diffusion model

<sup>b</sup>The values were estimated by fitting permeation data through whole skin to the two-layered diffusion model using previously obtained values of  $P_{ss}$  and  $K_{ss}$

**Fig. 3** Relationship between estimated and observed values for mean steady-state concentration of chemicals in whole (a) and stripped skin (b) of rat. The solid and dashed lines are the complete prediction and 95% confidence interval. Each point represents the mean  $\pm$  S.E. of 4 experiments.



There was an approximately 10-fold difference between LC and Dopa in terms of whole-skin permeation, but the difference in stripped-skin permeation remained within a few fold. Such features could be explained by a two-layered diffusion model, consisting of the first layer, the lipoidal stratum corneum, and the second layer, the viable epidermis and dermis (23,30). Skin permeation profiles of all chemicals through whole and stripped skin were fully described based on the two-layered and one-layered diffusion models, respectively, as shown in Figs. 1 and 2, and permeation parameters were obtained as listed in Table III.

Permeabilities through porcine skin were generally lower than those through rat skin (Figs. 1 and 2, Table III). The difference between the two animals for hydrophilic permeants was larger than that for lipophilic ones. The permeability coefficient through stripped skin of pig was low compared with that of rat. A similar tendency was observed upon comparison between human and hairless rat skin (32,33). The permeation properties of porcine skin do not completely accord with those of human skin (32). However, skin permeation of at least two kinds of animal could be explained by the two-layered diffusion model, which suggests that the same strategy is applicable to human skin permeation analysis.

The mean concentrations of chemicals in whole and stripped skin of rats and pigs during steady-state permeation were estimated based on the diffusion model used in skin permeation analysis. This method succeeded in predicting the skin concentration of most of chemicals tested (Figs. 3 and 4), reconfirming that rat and porcine skin can be considered as two-layered membranes and that the concentration of chemicals can be theoretically determined using permeation parameters. These results also suggest that the permeation experiment is useful to estimate the skin concentration.

Skin concentrations of Epi and Dopa were underestimated by the present method and the deviation from complete prediction in whole skin was larger than that in stripped skin in both animals (Figs. 3 and 4). These drugs may permeate skin *via* the aqueous porous pathway (34,35) or *via* appendages, such as sweat glands and hair follicles (36,37), due to their polarity. The contribution of such pathways should be taken into account in order to estimate the skin concentration of hydrophilic chemicals. On the other hand, skin concentration of CAF, which has the similar hydrophilicity to two drugs, was well predicted. These drugs are basic compounds and dissociate in the donor solutions (see “Preparation of donor solutions”, Table I). A citrate buffer of pH 5 was used in the permeation experiments of Epi and Dopa for a sufficient

**Fig. 4** Relationship between estimated and observed values for mean steady-state concentration of chemicals in whole (a) and stripped skin (b) of pig. The solid and dashed lines are the complete prediction and 95% confidence interval. Each point represents the mean  $\pm$  S.E. of 4 experiments.

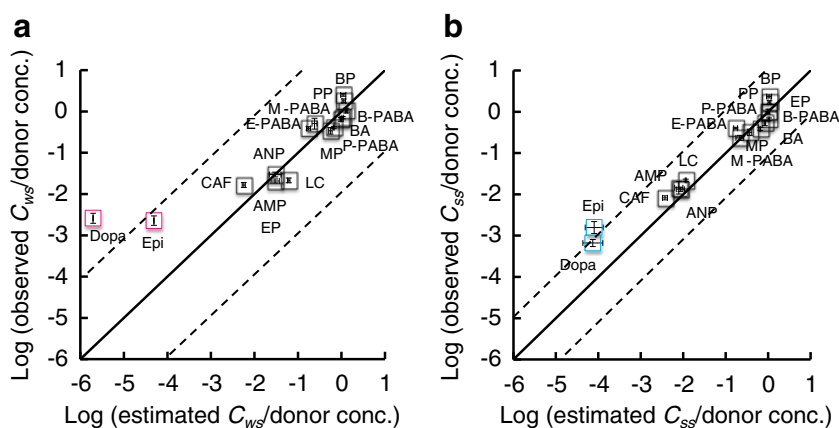
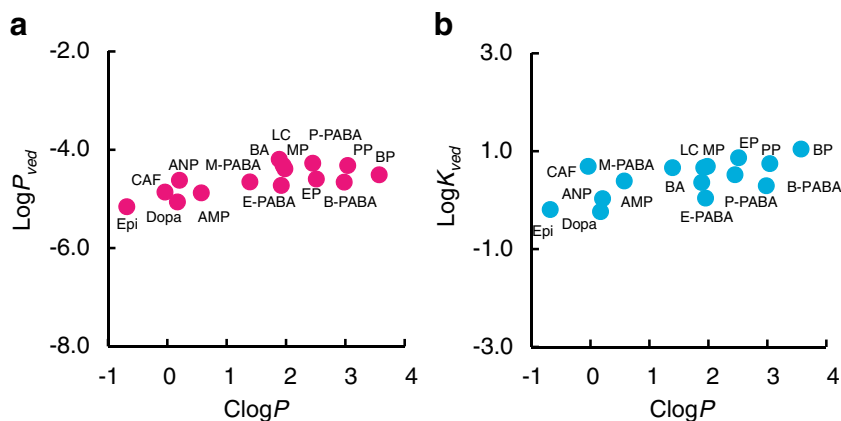


**Fig. 5** Relationship between permeation parameters of rat skin and  $\text{Clog}P$  of chemicals. **(a)** Permeability coefficient through stripped skin ( $P_{ss}$ ). **(b)** Stripped skin/donor vehicle partition coefficient ( $K_{ved}$ ). Each point represents the mean  $\pm$  S.E. of 4 experiments.



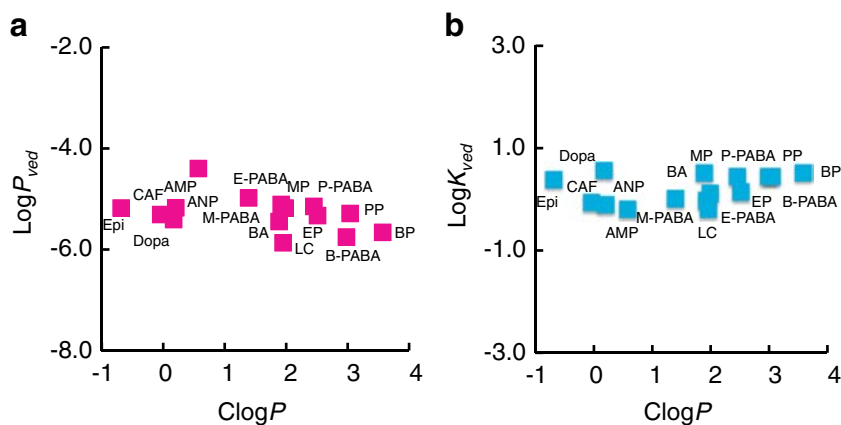
degree of dissociation, which would provide a pH gradient across skin. The pH gradient would allow both ionized and unionized species to be in the skin, whereas the permeability coefficient would be determined by the permeation of unionized species. In the experiment of CAF, a phosphate buffer of pH 7.4 was used and thus the drug completely dissociated in skin. The difference in donor pH might cause the difference in predictability among these drugs. It is only a speculation and further study will be required.

Skin concentrations following dermal exposure to chemicals can be estimated if only the skin permeation can be measured. However, it is not always possible to do this, especially for human skin, so the final goal is accurate prediction without experimental measurement. In the present study, permeation parameters of permeability coefficient and partition coefficient were used to calculate the skin concentration of chemicals, and such parameters can fortunately be estimated from physicochemical parameters. The permeation parameters for whole skin have already been reported to be related to  $\log P$  by us (22,31) and other investigators (4–10). The high dependence of whole skin permeation on the permeant lipophilicity has been recognized to reflect the properties of stratum corneum, the rate limiting and lipophilic layer (19). Systemic exposure after the absorption of chemicals by the skin is fully assessed from  $\log P$  values on the

assumption that skin is a single layer membrane (4–10,22,31). However, the viable epidermis and dermis cannot be ignored in assessment of skin concentration of chemicals, because they have large volume in skin and are the sites of action in some cases. It is necessary to estimate not only permeation parameters for whole skin (stratum corneum) but also those for stripped skin (viable epidermis and dermis) as shown by Eqs. 1 and 2. The permeability coefficient and partition coefficient for stripped skin of rats and pigs were almost constant, independent of the  $\text{Clog}P$  of chemicals (Figs. 5 and 6). The features were similar to the permeation behavior through poly(2-hydroxyethyl methacrylate) (pHEMA) membrane (22) and may be caused by the fact that aqueous vehicles were used in the permeation experiments.

Skin is made of two principal layers, epidermis and dermis. The outermost layer of the epidermis referred to as the stratum corneum consists of several layers of completely keratinized, dead cells and intercellular lipids, whereas the rest of the epidermis consists of keratinocytes, which secrete keratins and lipids like ceramides (38). The dermis contains mostly fibroblasts secreting collagen, elastin and ground substances, and the extracellular matrix composed of collagen fibrils, microfibrils and elastic fibers, embedded in proteoglycans (39). In spite of the different cell compositions, viable epidermis and dermis are highly hydrophilic compared with stratum

**Fig. 6** Relationship between permeation parameters of porcine skin and  $\text{Clog}P$  of chemicals. **(a)** Permeability coefficient through stripped skin ( $P_{ss}$ ). **(b)** Stripped skin/donor vehicle partition coefficient ( $K_{ved}$ ). Each point represents the mean  $\pm$  S.E. of 4 experiments.





corneum. Therefore, the permeation parameters from aqueous vehicles for viable epidermis and dermis might be insensitive to the lipophilicity of permeants. The range of molecular weight of permeants was relatively narrow (about twofold), so the effect of permeability coefficient could not be detected.

Anyway, the mean skin concentration of chemicals during steady-state permeation can be estimated using the prediction equations for permeation parameters without *in vitro* permeation experiment. For example, the permeation parameter values of LC for rat whole skin are calculated as  $P_{\text{ves}} = 3.28 \times 10^{-6} \text{ cm/s}$  and  $K_{\text{sc}} = 10.6$  from *ClogP* value (= 1.40) using equations previously reported (8,22). If the corresponding parameter values for stripped skin equal the mean values of all chemicals tested in this study,  $P_{\text{ss}} = 2.93 \times 10^{-5} \text{ cm/s}$  and  $K_{\text{ss}} = 3.76$  (Fig. 5). Introducing these values together with layer thickness ones into Eq. 1,  $\overline{C_{\text{ves}}}/C_v = 0.352$ , which is close to observed value of 0.530. Skin concentrations of other chemicals are also predictable in the same way. Only *ClogP* value of interested chemical is required for the prediction. The *in silico* estimation of skin concentration can be further applied to human, since the prediction equations for permeation parameters of human skin have been already available (4–6,8,9,31). The estimated values are the ratio against the donor concentrations of chemicals and thus vary depending on vehicles used in the donor solution. The permeation parameters from vehicles other than aqueous buffers for stripped skin may depend on the lipophilicity of chemicals. However, the values multiplied by the corresponding solubility will become constant independent of vehicles unless they affect the barrier function of skin, resulting from the maximum thermodynamic activity of chemicals (40). Provided that the maximum skin concentration was once obtained, the values from donor vehicles with various chemical concentrations can be predicted.

## CONCLUSION

In the present study, we successfully predicted the skin concentration following dermal exposure to chemicals with extensive polarity using permeation parameters obtained from a permeation experiment. As the method is based on Fick's law of diffusion, it can eventually be applied to human skin as well as rat and porcine skin. The aqueous porous pathway should be included in evaluations of the stratum corneum in order to achieve more accurate prediction for highly polar permeants. Complete *in silico* estimation without experimental measurement can be expected because the permeation parameters used in the estimation have been related to *ClogP* for whole skin and were independent of lipophilicity for stripped skin. This present method should become a useful tool to assess the efficacy of topically applied drugs and

cosmetic ingredients, as well as the risk of chemicals likely to cause skin disorders and diseases.

**Conflict of interest** The authors declare that there are no conflicts of interest.

## REFERENCES

- Gupta H, Babu RJ. Transdermal delivery: product and patent update. *Recent Pat Drug Deliv Formul.* 2013;7(3):184–205.
- Prausnitz MR, Langer R. Transdermal drug delivery. *Nat Biotechnol.* 2008;26(11):1261–8.
- Taylor JS, Parrish JA, Blank IH. Environmental reactions to chemical, physical, and biologic agents. *J Am Acad Dermatol.* 1984;11(5 Pt 2):1007–19.
- Guy RH, Hadgraft J, Maibach HI. Percutaneous absorption in man: a kinetic approach. *Toxicol Appl Pharmacol.* 1985;78(1):123–9.
- Tojo K, Lee AC. A method for predicting steady-state rate of skin penetration in vivo. *J Invest Dermatol.* 1989;92(1):105–8.
- Potts RO, Guy RH. Predicting skin permeability. *Pharm Res.* 1992;9(5):663–9.
- Hatanaka T, Katayama K, Koizumi T, Sugibayashi K, Morimoto Y. In vitro-in vivo correlation of percutaneous absorption: isosorbide dinitrate and morphine hydrochloride. *Biol Pharm Bull.* 1994;17(6):826–30.
- Vecchia BE, Bunge AL. Evaluating the transdermal permeability of chemicals. In: Guy RH, Hadgraft J, editors. *Transdermal drug delivery systems*, revised and expanded. 2nd ed. New York: Marcel Dekker; 2002. p. 25–55.
- Polak S, Ghobadi C, Mishra H, Ahamadi M, Patel N, Jamei M, et al. Prediction of concentration-time profile and its inter-individual variability following the dermal drug absorption. *J Pharm Sci.* 2012;101(7):2584–95.
- Chen L, Han L, Saib O, Lian G. In silico prediction of percutaneous absorption and disposition kinetics of chemicals. *Pharm Res.* 2015;32(5):1779–93.
- Chang RK, Raw A, Lionberger R, Yu L. Generic development of topical dermatologic products: formulation development, process development, and testing of topical dermatologic products. *AAPS J.* 2013;15(1):41–52.
- Kiistala U. Suction blister device for separation of viable epidermis from dermis. *J Invest Dermatol.* 1968;50(2):129–37.
- Surber C, Wilhelm KP, Bermann D, Maibach HI. In vivo skin penetration of acitretin in volunteers using three sampling techniques. *Pharm Res.* 1993;10(9):1291–4.
- Surber C, Wilhelm KP, Hori M, Maibach HI, Guy RH. Optimization of topical therapy: partitioning of drugs into stratum corneum. *Pharm Res.* 1990;7(12):1320–4.
- Schaefer H, Stüttgen G, Zesch A, Schalla W, Gazith J. Quantitative determination of percutaneous absorption of radiolabeled drugs in vitro and in vivo by human skin. *Curr Probl Dermatol.* 1978;7:80–94.
- Rougier A, Dupuis D, Lotte C, Roguet R, Schaefer H. In vivo correlation between stratum corneum reservoir function and percutaneous absorption. *J Invest Dermatol.* 1983;81(3):275–8.
- Groth L. Cutaneous microdialysis. A new technique for the assessment of skin penetration. *Curr Probl Dermatol.* 1998;26:90–8.
- Lademann J, Meinke MC, Schanzer S, Richter H, Darvin ME, Haag SF, et al. In vivo methods for the analysis of the penetration

- of topically applied substances in and through the skin barrier. *Int J Cosmet Sci.* 2012;34(6):551–9.
19. Russell WMS, Burch RL. The principles of humane experimental technique. London: Methuen; 1959.
  20. Blank IH. Cutaneous barriers. *J Invest Dermatol.* 1965;45(4):249–56.
  21. Cleek RL, Bunge AL. A new method for estimating dermal absorption from chemical exposure. 1. General approach. *Pharm Res.* 1993;10(4):497–506.
  22. Hatanaka T, Inuma M, Sugibayashi K, Morimoto Y. Prediction of skin permeability of drugs. I. Comparison with artificial membrane. *Chem Pharm Bull.* 1990;38(12):3452–9.
  23. Sugibayashi K, Todo H, Oshizaka T, Owada Y. Mathematical model to predict skin concentration of drugs: toward utilization of silicone membrane to predict skin concentration of drugs as an animal testing alternative. *Pharm Res.* 2010;27(1):134–42.
  24. Machatha SG, Yalkowsky SH. Comparison of the octanol/water partition coefficients calculated by ClogP, ACDlogP and KowWin to experimentally determined values. *Int J Pharm.* 2005;294(1-2):185–92.
  25. Long WJ, Brooks AE, Biazzo W. Analysis of polar compounds using 100% aqueous mobile phases with agilent ZORBAX eclipse plus phenyl-hexyl and other ZORBAX phenyl columns. Santa Clara: Agilent Technologies; 2009.
  26. Thompson JE, Davidow LW. A practical guide to contemporary pharmacy practice: appendix H pK<sub>a</sub>'s of drugs and reference compounds. Philadelphia: Lippincott Williams & Wilkins; 2009.
  27. Tehan BG, Lloyd EJ, Wong MG, Pitt WR, Gancia E, Manallack DT. Estimation of pK<sub>a</sub> using semiempirical molecular orbital methods. Part 2: application to amines, anilines and various nitrogen containing heterocyclic compounds. *Quant Struct Act Relat.* 2002;21(5):473–85.
  28. Flynn GL, Dürrheim H, Higuchi WI. Permeation of hairless mouse skin II: membrane sectioning techniques and influence on alkanol permeabilities. *J Pharm Sci.* 1981;70(1):52–6.
  29. Klang V, Schwarz JC, Lenobel B, Nadj M, Auböck J, Wolzt M, et al. In vitro vs. in vivo tape stripping: validation of the porcine ear model and penetration assessment of novel sucrose stearate emulsions. *Eur J Pharm Biopharm.* 2012;80(3):604–14.
  30. Oshizaka T, Kikuchi K, Kadhum WR, Todo H, Hatanaka T, Wierzba K, et al. Estimation of skin concentrations of topically applied lidocaine at each depth profile. *Int J Pharm.* 2014;475(1-2):292–7.
  31. Simon GA, Maibach HI. The pig as an experimental animal model of percutaneous permeation in man: qualitative and quantitative observations—an overview. *Skin Pharmacol Appl Skin Physiol.* 2000;13(5):229–34.
  32. Morimoto Y, Hatanaka T, Sugibayashi K, Omiya H. Prediction of skin permeability of drugs: comparison of human and hairless rat skin. *J Pharm Pharmacol.* 1992;44(8):634–9.
  33. Huong SP, Bun H, Fourneron JD, Reynier JP, Andrieu V. Use of various models for in vitro percutaneous absorption studies of ultraviolet filters. *Skin Res Technol.* 2009;15(3):253–61.
  34. Hatanaka T, Manabe E, Sugibayashi K, Morimoto Y. An application of the hydrodynamic pore theory to percutaneous absorption of drugs. *Pharm Res.* 1994;11(5):654–8.
  35. Polat BE, Seto JE, Blankschtein D, Langer R. Application of the aqueous porous pathway model to quantify the effect of sodium lauryl sulfate on ultrasound-induced skin structural perturbation. *J Pharm Sci.* 2011;100(4):1387–97.
  36. Hueber F, Wepierre J, Schaefer H. Role of transepidermal and transfollicular routes in percutaneous absorption of hydrocortisone and testosterone: in vivo study in the hairless rat. *Skin Pharmacol.* 1992;5(2):99–107.
  37. Horita D, Yoshimoto M, Todo H, Sugibayashi K. Analysis of hair follicle penetration of lidocaine and fluorescein isothiocyanate-dextran 4 kDa using hair follicle-plugging method. *Drug Dev Ind Pharm.* 2014;40(3):345–51.
  38. McGrath JA, Eady RA, Pope FM. Anatomy and organization of human skin. In: Burns T, Breathnach S, Cox N, Griffiths C, editors. *Rook's textbook of dermatology.* 7th ed. Oxford: Blackwell Publishing; 2004. p. 3.1–7.
  39. Breitreutz D, Miranca N, Nischt R. Basement membranes in skin: unique matrix structures with diverse functions? *Histochem Cell Biol.* 2009;132(1):1–10.
  40. Higuchi T. Physical chemical analysis of percutaneous absorption process from creams and ointments. *J Soc Cosmet Chem.* 1960;11:85–97.